Journal of Materials Chemistry

Cite this: *J. Mater. Chem.*, 2012, **22**, 7331

www.rsc.org/materials

PAPER

Band structure engineering for low band gap polymers containing thienopyrazine†

Chi-Yang Chao,*[a] Chung-Hsiang Chao,[a] Lung-Pin Chen,[a] Ying-Chieh Hung,[b] Shiang-Tai Lin,[b] Wei-Fang Su[a] and Ching-Fuh Lin[c]

Received 24th May 2011, Accepted 6th February 2012
DOI: 10.1039/c2jm12312f

In this research, we demonstrated that the energy levels, including highest occupied molecular orbital (HOMO) and lowest unoccupied molecular orbital (LUMO), and the optical absorptions of low band gap conjugated copolymers, consisting of 3-hexylthiophene (3HT) as electron-donating units and 2,3-diethylthieno[3,4-*b*]pyrazine (ETP) as electron-accepting units, could be systematically tuned by adjusting the composition and the geometric structure of the copolymers. Four new copolymers comprising of 3HT and ETP in different molar ratios (from 1 : 1 to 4 : 1), named **P1–P4**, were designed and synthesized *via* Suzuki coupling. The positions of the hexyl side chains on 3HT were varied to adjust the co-planarity of the copolymers. The LUMO, ranging from −2.94 eV to −3.11 eV, was lowered monotonically with increasing ETP content, and the break of co-planarity along the main chain showed a trivial effect on the LUMO. By contrast, the HOMO (−4.74 eV to −4.88 eV) was controlled by both the composition and the geometric structure of the copolymer. **P2**, having a twisted geometric structure, possessed a lower HOMO and a larger band gap compared to the planar **P3**. Bimodal optical absorptions with a relatively stronger absorption at long wavelengths were observed for all polymers which are due to intramolecular charge transfer. Optical band gaps in solution, ranging from 1.27 eV to 1.76 eV, decreased with increasing ETP content in the copolymer except **P2** and the trend was consistent with the HOMO–LUMO gaps. The optical absorptions and the energy levels are further confirmed by theoretical calculations. Good co-planarity was also found to benefit the electrical conductivity of p-doped thin films. Our results suggested that tuning the composition and the geometric structure would be an effective molecular design strategy toward desired band structure for low band gap conjugated polymers based on thiophene and thienopyrazine derivatives.

1. Introduction

Conjugated polymers have been widely used for various applications including solar cells, light-emitting diodes (LEDs), and organic field-effect transistors. Bulk heterojunction solar cells using these polymers as photoactive materials have attracted extensive attention because of their potential to fabricate large-area, ultrathin, flexible devices at low cost through wet processing. So far, the power conversion efficiency of polymer solar cells is still below satisfactory owing to insufficient photon absorption as well as sub-optimal exciton dissociation and charge transportation in the photoactive layer. The amount of solar photons absorbed is governed by the optical band gap of the polymer, generally dominated by the difference between the highest occupied molecular orbital (HOMO) and the lowest unoccupied molecular orbital (LUMO); therefore, low band gap conjugated polymers are inevitably needed to enhance light harvesting. In addition, proper positioning of energy levels with respect to electron acceptors such as fullerene[1] and titanium dioxide[2,3] is critical to the performance of the solar cell. The LUMO of the polymer is suggested to be 0.3–0.4 eV above the LUMO of the acceptors to ensure effective charge separation.[4,5] On the other hand, the low-lying HOMO of the polymer would enlarge the discrepancy with respect to the LUMO of the electron acceptor to increase the open circuit voltage (V_{oc}) of the photovoltaic devices.[6,7] Therefore, the chemical structure of a successful low band gap polymer must be carefully designed to achieve optimized band structure.

One of the extensively studied strategies to achieve low band gap is to employ electron-rich and electron-deficient units in a polymer as the donor–acceptor (D–A) interaction could

[a]*Department of Materials Science and Engineering, National Taiwan University, Taipei 10617, Taiwan. E-mail: cychao138@ntu.edu.tw; Fax: +886-2-23634562; Tel: +886-2-33663898*
[b]*Department of Chemical Engineering, National Taiwan University, Taipei 10617, Taiwan*
[c]*Graduate Institute of Photonics and Optoelectroics, National Taiwan University, Taipei 10617, Taiwan*
† Electronic supplementary information (ESI) available. See DOI: 10.1039/c2jm12312f

increase intramolecular charge transfer (ICT) and decrease the bond length alternation. In principle, both HOMO and LUMO of the acceptor unit are lower than the corresponding levels of the donor. The alternating D–A copolymer would exhibit a HOMO governed by the donor and a LUMO dominated by the acceptor, resulting in a lowered band gap compared to the homopolymer of either the donor or the acceptor. While the band structure of a D–A copolymer could be feasibly adjusted by incorporating various donors and acceptors,[8–25] there is a lack of systematic design strategies for a polymer with desired energy levels due to the vast structure diversity of the repeating units and essentially unlimited number of possible D–A combinations.

Another class of non-typical D–A systems consists of one unit whose HOMO is lower and LUMO is higher than the corresponding levels of the other unit. One unique feature of such non-typical D–A systems is that the energy levels can be systematically tuned by adjusting the composition of the D/A repeating units. One outstanding example is the copolymers containing thienopyrazine (TP) or its derivatives. TP derivatives are among the mostly used electron accepting units in D–A systems for their strong electron withdrawing feature and capability to stabilize the quinoid form to significantly lower the LUMO to suppress the band gap.[26–33] The band gaps of the D–A copolymers comprising of TP derivatives are larger than that of the TP homopolymer but smaller than that of the corresponding homopolymer of donors such as thiophene and fluorene. Therefore, optimization of the band structure for suitable energy levels and band gap could be accomplished by adjusting the composition of the TP based copolymers. Cheng *et al.* synthesized a series of copolymers comprising thiophene (T) as electron donor and di-alkyl substituted thienopyrazine (TP) as electron acceptor in different molar ratios ranging from 1 : 1 to 4 : 1.[26] The band gap was as low as 1.1 eV for the copolymer with T : TP = 1 : 1. However, the lack of side substituent on thiophene resulted in low molecular weight and insolubility of the copolymers with T : TP greater than 3 : 1. Jenekhe *et al.* also prepared copolymers based on 3-dodecylthiophene and TP without side substituent; and the optical band gap was ~1.3 eV for the copolymer with T : TP = 2 : 1. Nevertheless, the copolymer with T : TP = 3 : 1 was also found to be insoluble.[27] Although the combination of TP derivatives and thiophene (T) (or alkylthiophene (AT)) was demonstrated to exhibit low optical band gaps, which could be varied by changing the molar ratio between T (or AT) and TP units, the insolubility prevented further understanding of the band structures and applicability to photovoltaic devices. Janssen *et al.* prepared copolymers with T : TP = 4 : 1 or 5 : 1 by alternatively coupling TP units and either quaterthiophene or quinquethiophene segments having two alkyl side chains in different positions.[28] The optical band gaps of these copolymers in solution were 1.5 eV to 1.6 eV, larger than those containing fewer thiophene units.[29–31] The position of side chains was also shown to affect the band gap and the current density generated in the photovoltaic devices. According to these reports, the band gap of a conjugated polymer could be affected by its chemical composition and geometric structure. Therefore, the influence of these factors on the energy levels and optical absorption of the polymer should be critical to band gap engineering toward optimal solar cell performance.

In this study, a series of conjugated copolymers consisting of 3-hexylthiophene (3HT) as electron-donating units and 2,3-diethylthieno[3,4-*b*]pyrazine (ETP) as electron-accepting units in different ratios were synthesized *via* Suzuki coupling to adjust the composition and to evaluate the corresponding effect on the energy levels. Each thiophene ring contains a hexyl side chain to ensure good solubility, which also allows for the acquirement of electrochemical and absorption properties of the copolymers as an individual molecule for systematic comparison. The positions of the hexyl groups on 3HT units were intentionally varied to alter the geometric structure. The chemical structures, molecular weights as well as the optical and electrochemical properties were characterized for the synthesized copolymers. Quantum chemical calculations were performed to obtain the simulated optical and energy levels. The results are applied to investigate the significance of the chemical composition and the geometric structure affecting the band structures of these copolymers. This study demonstrates a feasible and systematic molecular design strategy for TP-based low band gap polymers toward optimal HOMO, LUMO and optical absorption.

2. Experimental

2.1 Materials

Thiophene, *N*-bromosuccinimide (NBS), 1-bromohexane, 1-bromooctane, 3-bromothiophene, and Aliquat336 were purchased from Acros Organics. 4,4′-Di-*tert*-butyl-2,2′-dipyridyl (dtbpy), 2-isopropoxy-4,4,5,5-tetramethyl-1,3,2-dioxaborolane (*i*p-Bpin), pinacolborane (HBPin), [1,3-bis(diphenylphosphino)propane] dichloronickel ($Ni(dppp)Cl_2$), and tetrakis(triphenylphosphine) palladium ($Pd(PPh_3)_4$) were obtained from Aldrich Chemicals. Di-μ-methoxobis(1,5-cyclooctadiene) diiridium ($[Ir(OMe)(COD)]_2$) was purchased from Strem Chemicals. Tetrahydrofuran (THF) was dried over sodium/benzophenone and freshly distilled prior to use. Other materials were used as received. 3-Hexylthiophene (3HT) was synthesized according to the literature.[34]

2.2 Measurement and characterization

All new compounds were characterized by an Electron Impact-Mass Spectrophotometer (EI-MS, Finnigan TSQ 700) and ^1H NMR using a Bruker AVANCE 400 MHz spectrometer with d-chloroform as solvent. Molecular weights and polydispersity indices (PDI) of the polymers were determined by gel permeation chromatography (GPC) using a Viscotek module-350 system with polystyrene as standard and THF or 1,2,4-trichlorobenzene (TCB) as eluent. TGA measurement was performed on a Perkin-Elmer TGA-7 apparatus at a heating rate of 20 °C min^{-1} under nitrogen atmosphere. UV-vis absorption spectra were recorded on a JASCO V570 spectrometer at ambient temperature. TCB solutions with polymer concentrations less than 10^{-5} M and thin films spin-coated from the TCB solutions were used for UV-vis absorption measurements. Electrochemical cyclic voltammetry (CV) was performed on polymer thin films coated on the working electrode using a CH Instruments 611B potentiostat/galvanostat system with Pt disk, Pt plate, and Ag/Ag^+ electrode as the working electrode, counter electrode, and reference electrode, respectively, in a 0.1 mol L^{-1} tetrabutylammonium hexafluorophosphate (Bu_4NPF_6) acetonitrile solution. The electrical

conductivity of pristine and doped polymers was obtained from four-probe in-plane resistivity measurement on the spin-coated thin films using a Mitsubishi MCP-T410 electrometer. The doping process was performed by immersing the spin-coated thin films in a 1 M KI_3 solution for 24 h and the doped thin films were washed thoroughly with copious DI water and dried under vacuum before measurement. Polymer solar cells (PSCs) with an inverted structure were fabricated using ITO glass as the positive electrode and Ag as the negative electrode. The ITO substrate was first covered with ZnO, then the photoactive layer was deposited by spin coating a TCB solution of polymer and $PC_{71}BM$ with designated weight ratio. NiO was then deposited on top of the photoactive layer and followed by the deposition of Ag by vacuum evaporation at 3×10^{-4} Pa. The current–voltage measurement of the devices was conducted on a computer-controlled Keithley 2400 Sourcemeter unit. A xenon lamp with an AM 1.5 filter was used as the white-light source, and the optical power at the sample was 100 mW cm^{-2}.

2.3 Synthesis of monomers

The synthetic routes of monomers are outlined in Scheme 1.

2-(3-Hexyl-5-(4,4,5,5-tetramethyl-1,3,2-dioxaborolan-2-yl)thiophen-2-yl)-4,4,5,5-tetramethyl-1,3,2-dioxaborolane (M1). In a 25 mL three-neck flask, $[Ir(OMe)(COD)]_2$ (0.059 g, 0.089 mmol), HBPin (1.52 g, 11.88 mmol) were mixed in 10 mL dry *n*-hexane and stirred at room temperature. To the mixture, dtbpy (0.048 g, 0.178 mmol) dissolved in dry *n*-hexane was then added drop wise. Afterward, 3-hexylthiophene (1 g, 5.94 mmol) was added, and the resulting mixture was refluxed for 24 h. The crude product was purified by column chromatography using a co-solvent (ethyl acetate/hexane = 1/10 in v/v) and subsequently diaphanous compound, **M1**, was obtained by vacuum distillation under 1×10^{-3} torr. Yield = 75%.

^{1}H NMR ($CDCl_3$, ppm): δ 7.49 (s, 1H), 2.85 (t, J = 1.9 Hz, 2H), 1.58 (m, 2H), 1.31 (m, 30H), 0.88 (t, J = 1.7 Hz, 3H).

EI-MS: m/z = 420.3 (M^+), calculated formula weight = 420.22.

EA: calculated for C, 62.88; H, 9.11; S, 7.63. Found for C, 62.78; H, 9.40; S, 7.04%.

3-Hexyl-2-(3-hexylthiophen-2-yl)thiophene (B3HT). Grignard reagent was prepared by adding 2-bromo-3-hexylthiophene (1.0 g, 4.05 mmol) to a stirred suspension of magnesium powder (0.295 g, 12.1 mmol) in THF under argon. The resulting mixture was refluxed for 12 h. The Grignard reagent was then added *via* a cannula to a mixture of 2-bromo-3-hexylthiophene (1.5 g, 6.07 mmol) and $Ni(dppp)Cl_2$ (44 mg, 0.081 mmol) in anhydrous THF and the reaction mixture was refluxed for 24 h under argon. The crude product was purified by column chromatography using hexane as eluent and then by vacuum distillation at 200 °C under 1×10^{-3} torr to give the diaphanous product of **B3HT**. Yield = 30%.

^{1}H NMR ($CDCl_3$, ppm): δ 7.27 (d, J = 2.1 Hz, 2H), 6.97 (d, J = 2.1 Hz, 2H), 2.49 (t, J = 1.9 Hz, 4H), 1.55 (m, 4H), 1.25 (m, 12H), 0.85 (t, J = 1.7 Hz, 6H).

2-(4-Hexyl-5-(3-hexyl-5-(4,4,5,5-tetramethyl-1,3,2-dioxaborolan-2-yl)-thiophene-2-yl)thiophen-2-yl)-4,4,5,5-tetramethyl-1,3,2-dioxaborolane (M2). $[Ir(OMe)(COD)]_2$ (0.03 g, 0.045 mmol) and HBPin (0.765 g, 5.98 mmol) were mixed in 5 mL dry *n*-hexane and stirred at room temperature. To the above mixture, dtbpy (0.024 g, 0.089 mmol) dissolved in dry *n*-hexane was added drop wise. Afterward, 3-hexyl-2-(3-hexylthiophen-2-yl)thiophene (1 g, 2.99 mmol) was added, and the resulting mixture was refluxed for 24 h. The crude product was purified by column chromatography

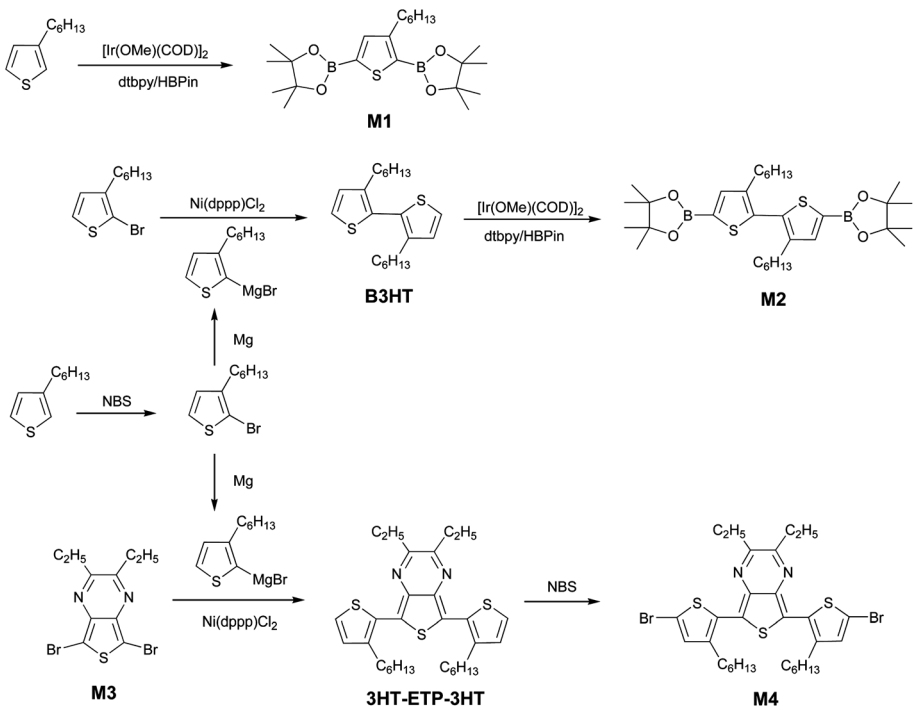

Scheme 1 Syntheses of monomers.

using a co-solvent (ethyl acetate/hexane = 1/10) and precipitation in methanol. The precipitates were collected by filtration and then vacuum dried to afford **M2** as white powders. Yield = 80%.

^{1}H NMR ($CDCl_3$, ppm): δ 7.50 (s, 2H), 2.49 (t, J = 2.0 Hz, 4H), 1.55 (m, 4H), 1.34 (s, 24H), 1.22 (m, 12H), 0.83 (t, J = 1.7 Hz, 6H).

EI-MS: m/z = 586.6 (M^+), calculated formula weight = 586.5.

EA: calculated for C, 65.33; H, 8.94; S, 10.93. Found for C, 65.52; H, 8.88; S, 10.26%.

5,7-Dibromo-2,3-diethylthieno[3,4-*b*]pyrazine (M3). 2,3-Diethylthieno[3,4-*b*]pyrazine (ETP) was prepared according to the literature.[35] The bromination of ETP by NBS afforded **M3**. Yield = 87%.

^{1}H NMR ($CDCl_3$, ppm): δ 2.96, 2.94 (q, J = 1.8 Hz, 4H), 1.39 (t, J = 1.8 Hz, 6H).

EI-MS: m/z = 350.1 (M^+), theoretical formula weight = 350.07.

EA: calculated for C, 34.31; H, 2.88; S, 9.16. N, 8.00. Found for C, 34.65; H, 2.95; S, 10.05, N, 8.22%.

2,3-Diethyl-5,7-bis(3-hexylthiophen-2-yl)thieno[3,4-*b*]pyrazine (3HT-ETP-3HT). The Grignard reagent of 2-bromo-3-hexylthiophene was prepared by adding 2-bromo-3-hexylthiophene (5.65 g, 22.9 mmol) to a stirred suspension of magnesium powder (0.83 g, 34.3 mmol) in THF under argon. The resulting mixture was refluxed for 12 h and then added *via* a cannula to a mixture of Br-ETP-Br (2 g, 5.71 mmol) and [1,3-bis(diphenylphosphino)propane]dichloronickel ($Ni(dppp)Cl_2$) (774 mg, 1.43 mmol) in anhydrous THF. The reaction was carried out at room temperature for 1 day under argon. The crude product was purified by column chromatography using a co-solvent (ethyl acetate/hexane = 1/15) and subsequently by recrystallization from methanol/methylene chloride gave dark red needles. Yield = 25%.

^{1}H NMR ($CDCl_3$, ppm): δ 7.36 (d, J = 1.3 Hz, 2H), 7.01 (d, J = 1.3 Hz, 2H), 2.95 (m, 8H), 1.72 (m, 4H), 1.25–1.5 (m, 18H), 0.88 (t, J = 1.8 Hz, 6H).

EI-MS: m/z = 524.3 (M^+), calculated formula weight = 524.85.

5,7-Bis(5-bromo-3-hexylthiophen-2-yl)-2,3-diethylthieno[3,4-*b*]pyrazine (M4). To a THF solution of **3HT-ETP-3HT** (0.96 g, 1.77 mmol), NBS (0.66 g, 3.71 mmol) in THF was added drop wise in the dark and the resulting solution was stirred at room temperature for 3 h. The reddish product was purified by column chromatography and recrystallization following a similar procedure as for the purification of **3HT-ETP-3HT** and murrey needles were obtained. Yield = 78%.

^{1}H NMR ($CDCl_3$, ppm): δ 6.95 (s, 2H), 2.98, 2.96 (q, J = 1.8 Hz, 4H), 2.89 (t, J = 2.0 Hz, 4H), 1.70 (p, J = 1.8 Hz, 4H), 1.25–1.5 (m, 18H), 0.89 (t, J = 1.8 Hz, 6H).

EI-MS: m/z = 682.4 (M^+), calculated formula weight = 682.64.

EA: calculated for C, 52.78; H, 5.61; S, 14.09; N, 4.1. Found for C, 53.09; H, 5.67; S, 13.20, N, 4.01%.

2.4 General procedure for Suzuki coupling

Equivalent amounts of dibrominated monomer (**M3** or **M4**) and diborated monomer (**M1** or **M2**) were added to a mixture comprising of anhydrous toluene and 2 M aqueous potassium carbonate in a 2/1 (v/v) ratio. Aliquat336 (2 mol%) and catalyst $Pd(PPh_3)_4$ (1 mol%) were added to the above mixture under argon and the resulting mixture was stirred for 72 h at 80 °C. The reaction mixture was then cooled to room temperature and slowly added to a vigorously stirred mixture of $MeOH/H_2O$ (v/v = 1/1) to afford precipitates as crude product. The solid was further purified by Soxhlet extraction with acetone and diethyl ether to remove oligomers and catalyst residues and was dried under reduced pressure at room temperature.

P1 was synthesized by reacting **M1** and **M3** to form greenish black solid. ^{1}H NMR ($CDCl_3$, ppm): δ 6.90–7.0 (m, 1H), 2.85–3.02 (m, 6H), 1.90–2.0 (m, 2H), 1.15–1.40 (m, 12H), 0.80–0.90 (m, 3H). **P2**, a purplish black solid, was obtained by reacting **M2** and **M3**. ^{1}H NMR (d-THF, ppm): δ 6.95–7.03 (m, 2H), 2.90–3.0 (m, 4H), 2.50–2.70 (m, 4H), 1.20–1.55 (m, 22H), 0.75–0.90 (m, 6H). **P3**, a murrey polymer, was synthesized by reacting **M1** and **M4**. ^{1}H NMR (d-THF, ppm): δ 7.03–7.18 (m, 3H), 2.85–3.10 (m, 8H), 2.58–2.63 (m, 2H), 1.74–1.82 (m, 4H), 1.20–1.60 (m, 26H), 0.80–0.92 (m, 9H). Dark red **P4** was synthesized using **M2** and **M4**. ^{1}H NMR (d-THF, ppm): δ 7.05–7.23 (m, 4H), 2.88–3.10 (m, 8H), 2.55–2.63 (m, 4H), 1.76–1.83 (m, 4H), 1.20–1.60 (m, 34H), 0.80–0.95 (m, 12H).

2.5 Theoretical calculation

The energy levels and optical properties of the polymers are also determined based on quantum chemical calculations using commercial package Gaussian 03.[36] The ground state structures were optimized by using density functional theory (DFT) with the B3LYP functional and the 6-31G* basis set.[37] It has been shown that B3LYP/6-31G* gives decent ground state structures of conjugated polymers. HOMO/LUMO energies and band gap are determined from single point energy calculations performed at B3LYP/6-31 + G* level. The calculations were performed for oligomers with the degree of polymerization of 1 to 4. The properties of the corresponding polymer were determined by linear extrapolation (using the inverse of the degree of polymerization) either to the degree of polymerization measured in experiment or to infinite. Optical absorption spectra of each polymer were represented by Gaussian line-broadening using the equation[38]

$$A(w) = \frac{1}{\sigma\sqrt{2\pi}} \sum_n h_n \exp \frac{-(w_n - w)^2}{\sigma^2}$$

where σ is FWHM (full width at half maximum) of the UV-vis absorption peak and ω_n and h_n are the absorption length and oscillator strength of the transition obtained from semiempirical ZINDO[39] calculations in which only singlet states were considered. The value of σ = 300 is chosen to spread the calculated ZINDO UV-vis spectrum. To investigate the effect of geometric structure on the energy levels of the polymers, we design two categories of copolymer (without and with side chain on thiophene) with different ratios of T : TP. For saving computational times, we replaced the hexyl substituent on 3-hexylthiophene with a methyl substituent and neglected the ethyl substituents on TP.

3. Results and discussion

3.1 Design and synthesis of copolymers

A series of copolymers containing 3HT and ETP (**P1–P4**) in different ratios were designed and synthesized in this work to systematically vary the compositions and the geometric structures. Thus, their energy levels and optical absorptions can be adjusted. Hexyl side chain is located on every thiophene unit and di-ethyl side groups are present on TP to ensure good solubility of the copolymers. The synthetic routes of monomers are outlined in Scheme 1. The syntheses and the chemical structures of the synthetic copolymers as well as the chemical structures of the analogous polymers for theoretical calculations are illustrated in Scheme 2. Note that the polymers named as **P1M–P4M** and **PMT** indicated that the 3-hexylthiophene units are replaced with 3-methylthiophene (MT) in the calculations, while all the side chains are removed for **P1X–P4X** and **PT**.

Different from the syntheses of most thiophene based copolymers *via* Stille coupling, Suzuki coupling was employed for environmental benignity by avoiding the use of tin-based reagents. The chemical structures and purity of all monomers were verified by ^{1}H NMR, Electron Impact-Mass Spectrophotometer (EI-MS) and elemental analysis (EA). To the best of our knowledge, di-borated 3-alkylthiophene (**M1**) was first synthesized in this work. Although many ligands and catalysts for boration have been reported,[31,40–42] only the iridium-based catalyst was successful in boration of both 2,5-position of 3-hexylthiophene in high yield (75%) due to very distinctive reactivity in 2- and 5-positions.

All the polymers synthesized could be dissolved in 1,2,4-trichlorobenznene (TCB). With increasing 3HT content, the copolymers, such as **P3** and **P4**, exhibited good solubility in chloroform and tetrahydrofuran, indicating that the hexyl side chains on thiophene would substantially enhance the solubility. Table 1 lists the weight average molecular weight (M_w) and the polydispersity index (PDI) of the copolymers obtained from high temperature gel permeation chromatography (GPC) operated at 130 °C using TCB as eluent to ensure thorough dissolving of the polymers. All the synthetic polymers exhibited moderate molecular weights (<10 000), suggesting that Suzuki coupling using thiophene-based borated monomers (**M1** and **M2**) might not be very effective. It was found that **P1** and **P2** synthesized from **M3** with Br on ETP exhibited relative low molecular weight, while **P3** and **P4** using **M4** with Br on 3HT showed enlarged numbers of repeating units. This might be attributed to weak reactivity of Br on ETP in **M3** due to the presence of strong electron withdrawing nitrogen. Stille coupling, employing trimethyl-tin decorated 3HT and **B3HT** to replace borated **M1** and **M2**, was performed as reference studies. The resulting **P1** and **P2** still exhibited relative low molecular weights (<2500), while apparently high molecular weights (>10 000) were observed for the corresponding **P3** and **P4**. These observations further

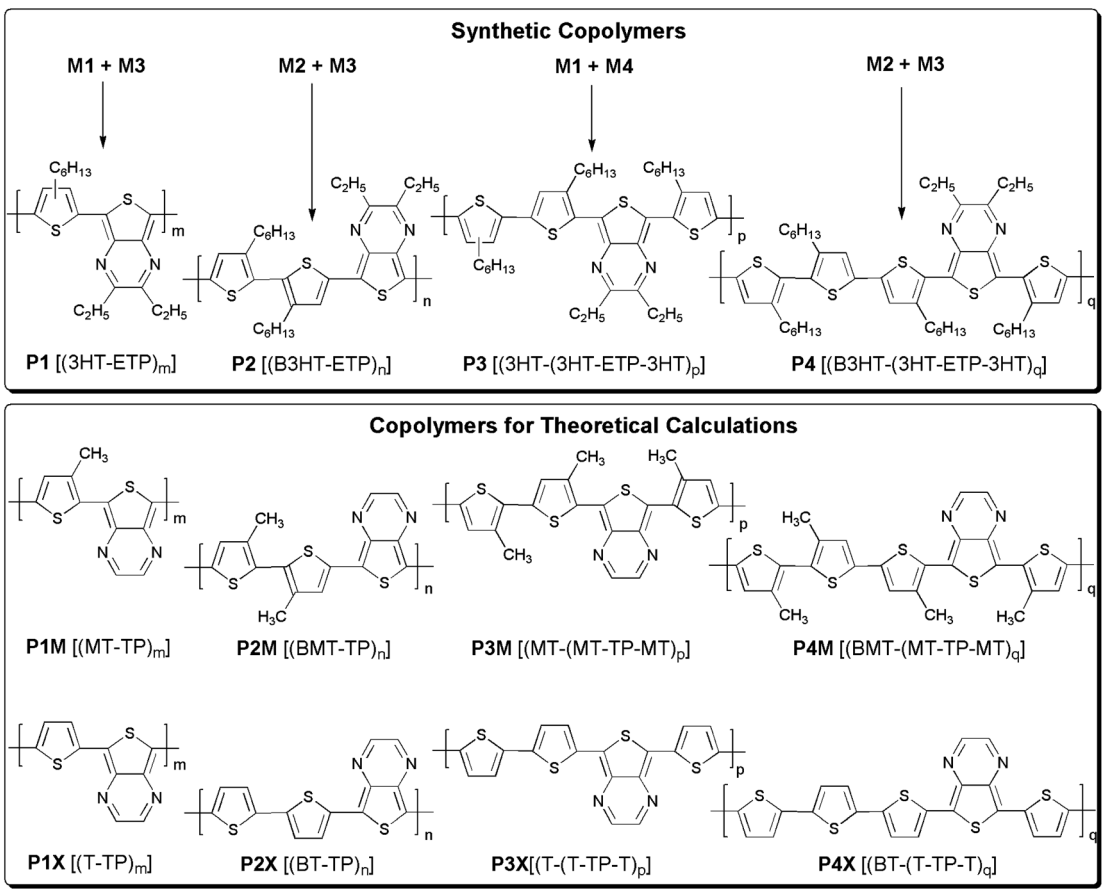

Scheme 2 Syntheses of copolymers and the analogous copolymers for theoretical calculations.

Table 1 Molecular weights and thermal properties of the synthetic polymers

Polymers	3HT : ETP (molar ratio)	Number of repeat units	Number of rings	M_w	PDI	T_d/°C
P1	1 : 1	5	10	1600	1.51	318
P2	2 : 1	7	21	3400	1.75	321
P3	3 : 1	8	32	5500	2.21	370
P4	4 : 1	9	45	7800	2.69	446

confirmed the low reactivity of **M3** and which should be responsible for the low molecular weights of **P1** and **P2**. Although the molecular weights of the obtained polymers were moderate, the optical absorptions and the energy levels of these polymers should be applicable to estimate optical absorption properties and energy levels of the corresponding polymers possessing high molecular weight. The general tendencies for HOMO and LUMO levels of the polymers with lower molecular weights and those of the polymers with infinite degree of polymerization are in accordance, as shown in the theoretical calculation discussed later.

All the copolymers exhibited a weight loss less than 5% upon heating to 300 °C as retrieved from TGA curves shown in Fig. S1†, suggesting good thermal stability. In general, the increment in 3HT content in the copolymer led to higher thermal decomposition temperature T_d, which might be attributed to the high co-planarity of **M4** and larger molecular weights resulting in better conjugation along the main chain to improve the thermal stability of **P3** and **P4**.

3.2 Molecular modeling for geometric structures of copolymers

To evaluate the influence of the geometric structure on the energy levels and optical absorptions of the synthetic copolymers **P1–P4**, molecular modeling of the analogous **P1M–P4M** was performed to retrieve the information of co-planarity of the main chain. MT, BMT and MT-TP-MT were adopted for the analogues of 3HT, **B3HT** and **3HT-ETP-3HT** as the building units respectively; while T, BT and T-TP-T were used for the counterparts without side substitutes for comparison. The optimized geometric structures of the repeat units $(MT\text{-}TP)_2$, $(BMT\text{-}TP)_1$, $(MT\text{-}(MT\text{-}TP\text{-}MT))_1$ and $(BMT\text{-}(MT\text{-}TP\text{-}MT))_1$ of **P1M–P4M**, as well as the corresponding units without methyl group on thiophene of **P1X–P4X** are shown in Fig. 1. As seen in Fig. 1(a) and (b), both $(MT\text{-}TP)_2$ and $(T\text{-}TP)_2$ show prefect planar structures, indicating that the presence of a methyl group in **P1M** should not affect the co-planarity. By contrast, owing to the steric hindrance of the two methyl groups on BMT, the co-planarity of $(BMT\text{-}TP)_1$ between the two thiophene rings in BMT is broken to result in the dihedral angle $\phi_2 = 124.9°$, as shown in Fig. 1(c). Nevertheless, without the methyl group, the calculated dihedral angle ϕ_2 of $(BT\text{-}TP)_1$ is 179.9° (Fig. 1(d)). Similar to $(MT\text{-}TP)_2$ and $(T\text{-}TP)_2$, the break of co-planarity is neither observed in $(MT\text{-}(MT\text{-}TP\text{-}MT))_1$ (Fig.1(e)) nor in $(T\text{-}(T\text{-}TP\text{-}T))_1$ (Fig. 1(f)). Meanwhile, $(BMT\text{-}(MT\text{-}TP\text{-}MT))_1$ exhibits a remarkable twist in BMT (Fig. 1(g)), whereas $(BT\text{-}(T\text{-}TP\text{-}T))_1$ (Fig. 1(h)) retains a good co-planarity. From the geometric structure studies, we could expect **P1** and **P3** employing **M1** as co-monomer to exhibit a strong co-planarity. By contrast, **P2** and **P4** which adopted **M2** as a co-monomer should have a twisted main chain. In addition, **P4** would exhibit a better co-planarity than **P2** since the significant twist along the main chain occurs with every 5 rings for **P4** while that occurs with every 3 rings for **P2**.

3.3 Optical properties

The UV-Vis absorption spectra of copolymers in TCB solution and in solid state are shown in Fig. 2(a) and (b) respectively. All the copolymers show bimodal absorptions, where ETP or **3HT-ETP-3HT** units correspond to the short wavelength absorptions while the intramolecular charge transfer (ICT) contributed by the donor–acceptor effect is responsible for the longer wavelength absorptions. The λ_{max} and the optical band gaps of synthesized copolymers are summarized in Table 2. All the copolymers show lower optical band gaps compared to pristine P3HT.

As seen in Fig. 2(a) illustrating the UV-Vis spectra in TCB solution, the increment in ETP content leads to a red shift in λ_{max}, except **P2** showing the smallest λ_{max}. In addition, **P1**, **P3** and **P4** exhibit stronger absorptions at long wavelengths whereas **P2** possesses a more pronounced absorption at short wavelengths. Also shown in Table 2, increasing the ETP content in the copolymers reduces the energy gap despite that $E_{g,opt}$ of **P3** is smaller than that of **P2**. In general, increasing the ETP content is expected to enhance the ICT to lower the band gap and to promote the absorptions at long wavelengths. Therefore, the unexpected larger band gap and weaker red absorptions of **P2** are believed to be associated with the significant break of co-planarity in **P2**, resulting in the suppression of ICT.

Regarding the absorptions of thin films depicted in Fig. 2(b), intermolecular energy transfer results in broader and red-shifted absorption peaks, as compared with the absorptions in solution. The red shifts of λ_{max} are more provoked for **P1** and **P3** than those for **P2** and **P4**, suggesting that the former two might exhibit more organized packing in the thin films than the latter two. Therefore, we might infer that the good co-planarity in **P1** and **P3** should lead to more ordered arrangement in solid state and the irregular orientation of hexyl side chains would not severely interrupt the inter-chain organization; while the break of co-planarity in **P2** and **P4** originated from the **B3HT** unit could result in less ordered packing despite the better control on the orientation of hexyl side chains.

Fig. 3 shows the calculated UV-vis spectra by ZINDO calculations. Since the intensity of the UV-vis spectrum depends on the chain length, the calculations were performed using polymers with the same number of rings. We choose 20 rings for all the polymers except **P2M** and **P2X** (21 rings). The calculated spectra are generally in good agreement with experimental results regarding the optical band gaps. In Fig. 3(a), increasing TP content in **P1X–P4X** without methyl substituent on thiophene results in a monotonic red shift, in agreement with the aforementioned expectation. By contrast, the ICT absorption for **P2M** with methyl substituent on thiophene shows a blue shift compared to **P3M** in Fig. 3(b), in consistency with the measured spectra for **P2** and **P3**. The study of simulated spectra further supports the previous argument stating that the particular large

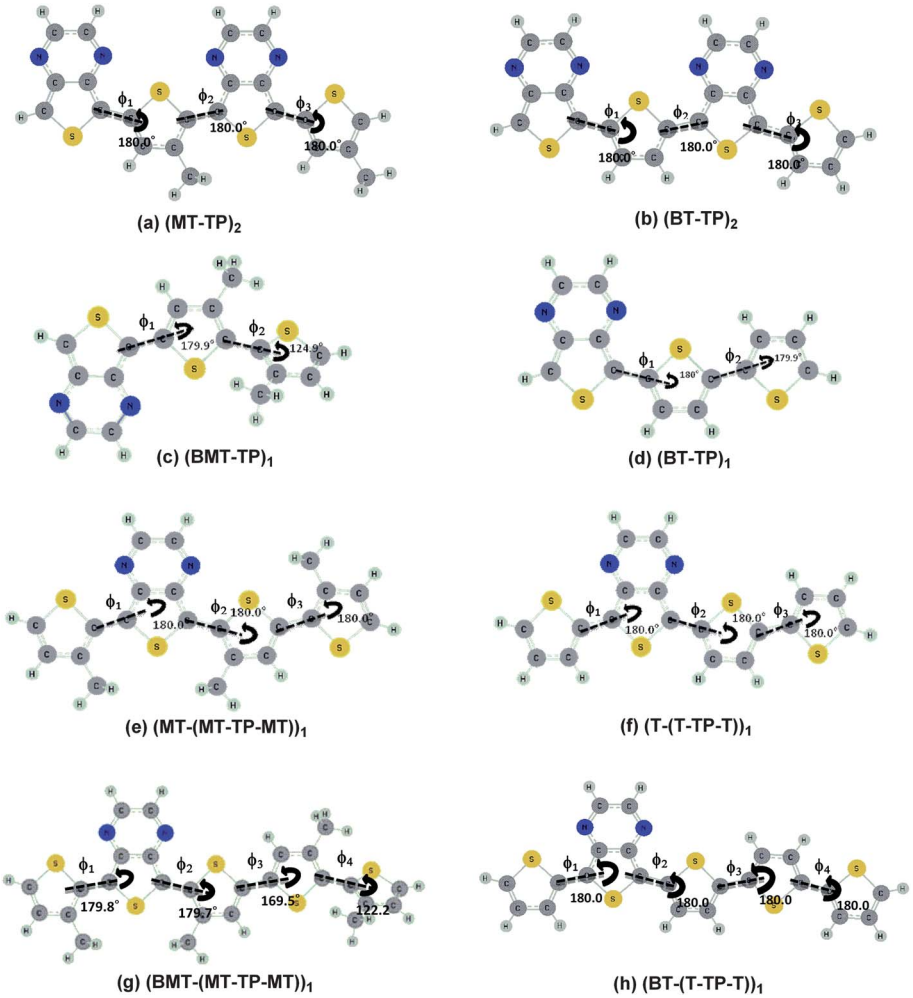

Fig. 1 Optimized structures at B3LYP/6-31G* of (a) $(MT\text{-}TP)_2$, (b) $(T\text{-}TP)_2$, (c) $(BMT\text{-}TP)_1$, (d) $(BT\text{-}TP)_1$, (e) $(MT\text{-}(MT\text{-}TP\text{-}MT))_1$, (f) $(T\text{-}(T\text{-}TP\text{-}T))_1$, (g) $(BMT\text{-}(MT\text{-}TP\text{-}MT))_1$, (h) $(BT\text{-}(T\text{-}TP\text{-}T))_1$.

optical band gap of **P2** should originate from the severe break of co-planarity in **P2**.

3.4 Electrochemical properties and energy levels

The electrochemical properties of the polymers, investigated by cyclic voltammetry (CV), are listed in Table 2. All copolymers exhibited partial reversibility in both n-doping and p-doping processes as shown in Fig. 4. From the values of $E_{ox,onset}$ and $E_{red,onset}$, HOMO and LUMO as well as the electrochemical band gap ($E_{g,cv}$) of the polymers could be obtained according to the following equations:

$$\text{HOMO} = -4.8 - E_{ox,onset}$$

$$\text{LUMO} = -4.8 - E_{red,onset}$$

$$E_{g,cv} = \text{LUMO–HOMO}$$

The band gaps retrieved from the electrochemical method exhibit a trend similar to the optical band gaps with respect to the composition of the copolymer; nevertheless, the $E_{g,cv}$ is systematically larger than $E_{g,opt}$ probably due to the barriers for charge transfer between the electrodes, the polymer films and the supporting electrolyte, resulting in lags between voltage input and current measurement.

The increment in ETP content would lower the LUMO because of strong electron accepting feature of ETP enabling feasible entrance of electrons into LUMO, which is in accordance with the general agreement that LUMO should be mainly determined by electron acceptor in a D–A copolymer.[8,24,43–47] However, the HOMO is elevated with increasing ETP in the copolymer, contradictory to the common statement declaring that the HOMO should be governed by the electron donating unit. Recently, Janssen *et al.* suggested that TP derivatives should be both good electron acceptors and electron donors in comparison with thiophene, allowing the particular small band gap of thiophene–TP copolymers as a result of lowered LUMO and lifted HOMO.[48] It is also noticed that HOMO of **P2** is lower than HOMO of **P3**, as a consequence of the twisted main chain of **P2**. Hence, we suggest that the position of HOMO should be determined by both the TP content and the geometric co-planarity whereas the level of LUMO is governed by the TP content, which will be further confirmed by the theoretical calculation discussed later. It is worthy to point out that the

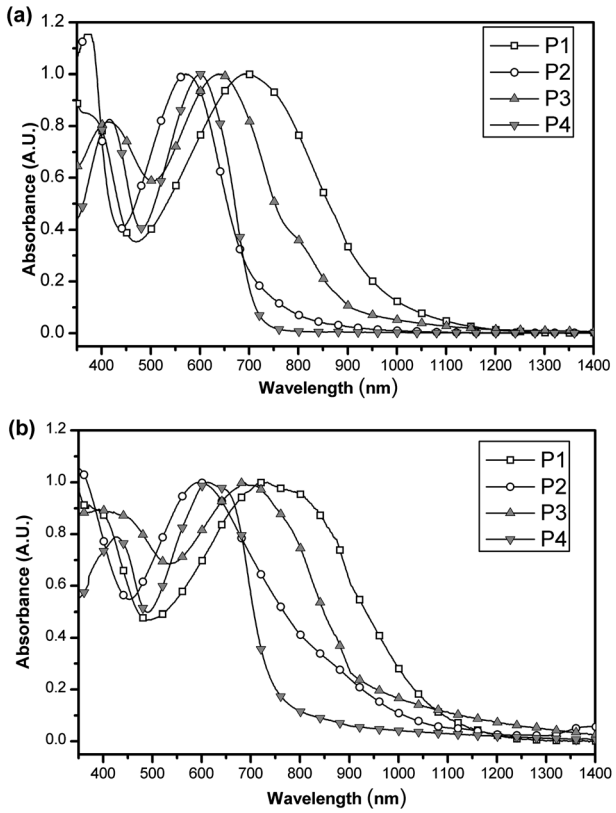

Fig. 2 Normalized optical absorption spectra of copolymers (a) in TCB solution and (b) in solid state.

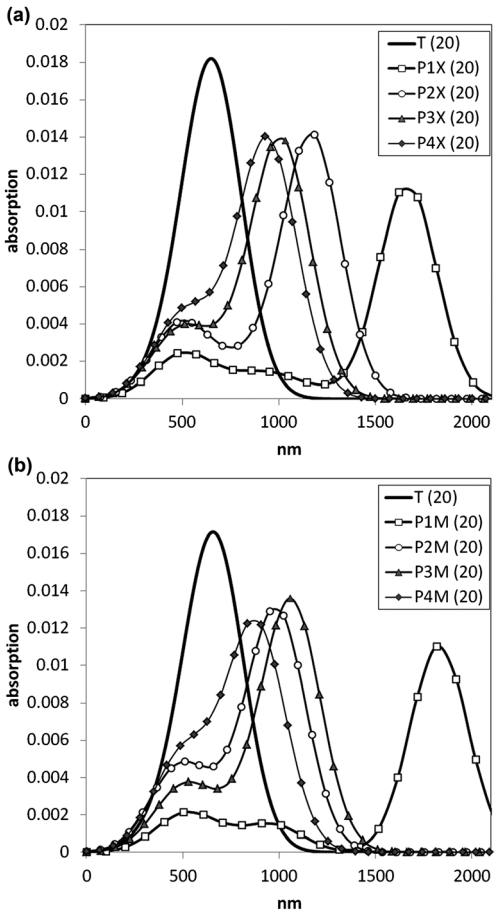

Fig. 3 Simulated UV-vis absorptions for copolymers with the number of rings = 20 (21) by ZINDO calculation: (a) **P1X–P4X** and **PT** (represented by T(20)) without methyl substituents on thiophene and (b) **P1M–P4M** and **PMT** (represented by T(20))with methyl substituents on thiophene.

reduction in LUMO is more notable than the elevation of HOMO; in addition, the small content of ETP (20 mol%) in **P4** could significantly lower the LUMO but slightly lift the HOMO.

Table 3 summarizes the calculated properties of **P1M–P4M** and **P1X–P4X**, including HOMO, LUMO, and band gaps (H–L and ZINDO) based on the degree of polymerization of the corresponding synthetic polymers **P1–P4**. The general trends of the calculated energy levels are in good agreement with the experimental observations. The calculated HOMO–LUMO gaps are consistently lower than the experimental band gaps from cyclic voltammetry measurement by about 0.3 eV (0.34, 0.42, 0.33, 0.34 for **P1M–P4M** (MT : TP = 4 : 1 to 1 : 1) respectively). The band gaps obtained from ZINDO calculations are in general lower than the calculated HOMO–LUMO gaps by about 0.2 eV (0.27, 0.21, 0.20, 0.24 for **P1M–P4M** (MT : TP = 4 : 1 to 1 : 1) respectively).

Fig. 5(a) shows the energy levels obtained from the theoretical calculations for **P1M–P4M** and **PMT** as well as those from experimental results of **P1–P4** and **P3HT**. The degree of polymerization (DP_n) of **P1M–P4M** and **PMT** used for calculation are equal to the DP_n of corresponding **P1–P4** and **P3HT**, and these DP_n are denoted as experimental DP_n. The LUMO levels of **P1M–P4M** are found to decrease with the decrement of MT content; while the HOMO levels show an irregular variation with respect to the MT content. The changes of energy levels are in concurrence with the experimental observation for **P1–P4**. Fig. 5(b) shows the calculated energy levels of **P1M–P4M** and

Table 2 Optical and electrochemical properties of **P1–P4**

	Optical absorption				Electrochemical property				
	In solution		Thin film		Oxidation		Reduction		
Polymer	λ_{max}/nm	$E_{g,opt}$/eV	λ_{max}/nm	$E_{g,opt}$/eV	E_{onset}/V	HOMO/eV	E_{onset}/V	LUMO/eV	$E_{g,cv}$/eV
P1	380, 690	1.27	375, 730	1.14	−0.06	−4.74	−1.69	−3.11	1.63
P2	381, 565	1.44	387, 580	1.24	0.02	−4.82	−1.74	−3.06	1.76
P3	422, 635	1.37	420, 690	1.33	−0.04	−4.76	−1.78	−3.02	1.74
P4	425, 595	1.75	423, 610	1.65	0.08	−4.88	−1.86	−2.94	1.94

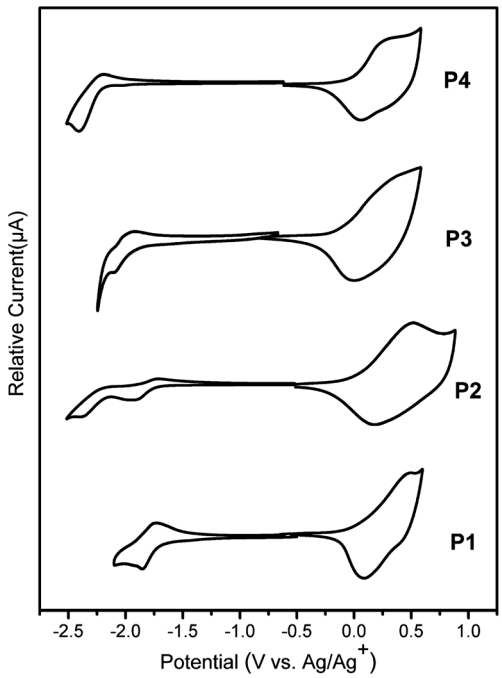

Fig. 4 Cyclic voltammograms of the polymer thin films on platinum electrode in a 0.1 mol L^{-1} Bu_4NPF_6 acetonitrile solution.

PMT with experimental DP_n as well as those of **P1M–P4M** and **PMT** with infinite DP_n. The variations in HOMO and LUMO with respect to the content of MT for the samples having relative low molecular weight and those for high molecular weight counterparts are in good consistency, and the discrepancy originating from the differences in chain lengths is small for **P3M** and **P4M**. This observation suggested that the optical and electrochemical properties of **P1–P4** with moderate molecular weights should be applicable to describe the energy levels of the analogous polymers with high molecular weight.

Fig. 5(c) illustrates the calculated energy levels for **P1M–P4M** and **PMT** with experimental DP_n as well as those for **P1X–P4X** and **PT** with experimental DP_n. For **P1X–P4X**, both HOMO and LUMO levels vary monotonically and the band gap decreases with the increment of TP content. It is noticed that the polymers containing methyl groups (**P1M–P4M**) possess LUMO systematically higher than the counterparts without methyl groups (**P1X–P4X**) because of the electron-donating nature of methyl group. Nevertheless, only **P1M** and **P3M** exhibit higher HOMO compared to **P1X** and **P3X** respectively while **P2M** and **P4M** show HOMO similar to those of **P2X** and **P4X** despite that HOMO of **P1M–P4M** are expected to be systematically higher than those of **P1X–P4X**. In addition, the TP containing **P4M** would even lower the HOMO as compared to **PMT**, while the HOMO of **P4X** was higher than that of **PT**. Hence, the HOMO is suggested to be elevated by increasing the TP content but it could be significantly lowered by the break of co-planarity, resulting in irregular variation of HOMO levels with respect to the 3HT (or MT) contents. The effect of geometric structure could be also applicable to explain the particular large band gap of **P2** and **P2M** as seen in Fig. 5(a).

Table 3 Calculated HOMO, LUMO and band gaps (H–L and ZINDO)

Polymer	HOMO/ eV	LUMO/ eV	E_g (H–L)/ eV	E_g (ZIN)/ eV
P1M [$(MT\text{-}TP)_5$]	−4.57	−3.28	1.29	1.02
P1X [$(T\text{-}TP)_5$]	−4.70	−3.43	1.27	1.03
P2M [$(BMT\text{-}TP)_7$]	−4.63	−3.20	1.43	1.23
P2X [$(BT\text{-}TP)_7$]	−4.64	−3.37	1.27	1.10
P3M [$(MT\text{-}(MT\text{-}TP\text{-}MT))_8$]	−4.44	−3.12	1.32	1.13
P3X [$(T\text{-}(T\text{-}TP\text{-}T))_8$]	−4.66	−3.33	1.33	1.19
P4M [$(BMT\text{-}(MT\text{-}TP\text{-}MT))_9$]	−4.62	−3.02	1.60	1.34
P4X [$(BT\text{-}(T\text{-}TP\text{-}T))_9$]	−4.69	−3.3	1.38	1.24
PMT [$(MT)_{120}$]	−4.52	−2.61	1.91	1.67
PT [$(T)_{120}$]	−4.76	−2.90	1.86	1.66

In order to understand the origins for the significant influence of break of co-planarity on HOMO, we calculated the frontier orbitals of the copolymers to extract the distribution of π-electrons at HOMO and LUMO. Fig. 6 illustrates the frontier orbitals of **P2M** [$(BMT\text{-}TP)_7$] and **P3M** [$(MT\text{-}(MT\text{-}TP\text{-}MT))_5$]. For both molecules, the frontier orbitals of HOMO spread over all the MT units and the thiophene ring of the TP uniformly, but the charge density is more localized on the pyrazine ring of TP for the LUMO orbitals. The localization of π-electrons on TP would make the bonding character between two neighboring MT the weakest among all the inter-ring bondings when the polymer is at LUMO; whereas, the uniform distribution of π-electrons along the main chain should lead to similar bonding characters in all inter-ring bondings when the polymer is at HOMO. Therefore, the deviation from co-planarity might strongly affect the inter-ring conjugation to influence the HOMO; by contrast, the change in the inter-ring dihedral angles should have little impact on the LUMO. As a summary, the energy levels of the thiophene–TP system could be affected by both the composition and the geometric structure, and the latter would exhibit a more pronounced effect on the HOMO to enlarge the band gap.

3.5 Electrical conductivity and photovoltaic performances

No electrical conductivity could be detected for all pristine polymer thin films before doping, which should be reasonable since these polymers are intrinsic semiconductors. The conductivities of the doped films were 1.76×10^{-5}, 5.28×10^{-5}, 9.6×10^{-4} and 8.9×10^{-4} S cm^{-1} for **P1**, **P2**, **P3** and **P4** respectively. The low conductivity of **P1** and **P2** could be attributed to the relative low molecular weight, leading to short conjugation lengths and poor π–π stacking as suggested by the limited red shift of optical absorptions in solid state. Dramatic increment in electrical conductivity was observed for **P3** and **P4** as compared to **P1** and **P2** due to the increment in molecular weight. It was noticed that the conductivity of **P3** was higher than that of **P4** despite that the chain length of **P4** was longer, suggesting that the good co-planarity in **P3** should benefit the charge transportation because of the elongation of conjugation and the improvement in interchain packing according to the noticeable red shift in λ_{max} of **P3**.

Bulk heterojunction (BHJ) photovoltaic cells based on **P4** and $PC_{71}BM$ in different weight ratios were fabricated and evaluated. **P4** was adopted for their low-lying HOMO and relative high molecular weight among **P1–P4**. The devices were constructed in an ITO/ZnO/polymer:$PC_{71}BM$/NiO/Ag assembly as an inverted structure for better stability. Open circuit voltage (V_{oc}), short

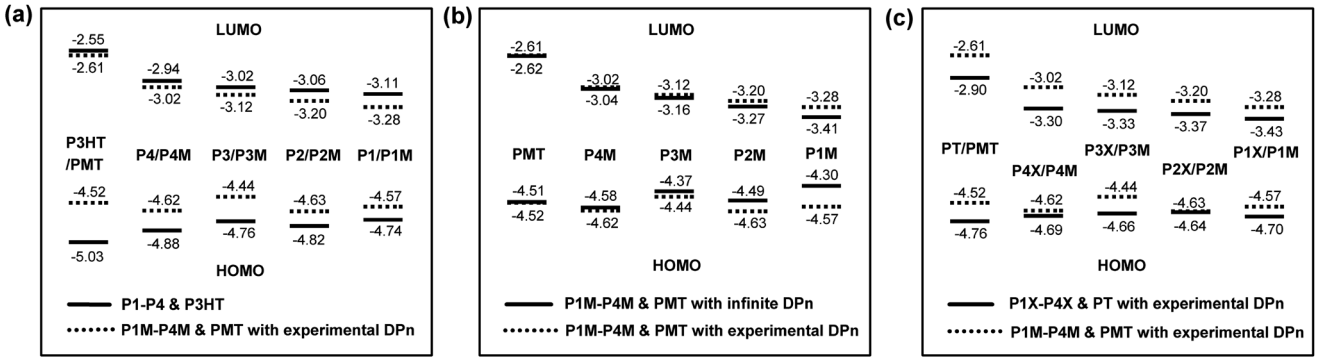

Fig. 5 Comparison of HOMO and LUMO energy levels for (a) **P1–P4** and **P3HT** obtained from cyclic voltammograms as well as **P1M–P4M** and **PMT** with experimental DP_n from theoretical calculations; (b) **P1M–P4M** and **PMT** with different DP_n from calculations; and (c) **P1M–P4M** and **PMT** with experimental DP_n as well as **P1X–P4X** and **PT** with experimental DP_n from calculations.

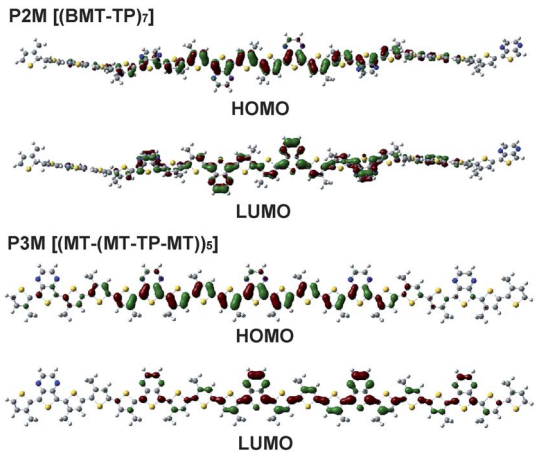

Fig. 6 Frontier orbitals of **P2M** and **P3M**.

Table 4 Photovoltaic properties of the cells using the blends of P4 and $PC_{71}BM$ for active layer under the illumination of AM 1.5, 100 mW cm^{-2}

Weight ratio of P4 : $PC_{71}BM$	V_{OC}/V	J_{SC}/mA cm^{-2}	FF (%)	PCE (%)
1 : 1	0.49	2.08	32.9	0.34
1 : 4	0.45	4.15	37.4	0.70

circuit current (J_{sc}), fill factor (FF), and power conversion efficiencies (PCE) are summarized in Table 4. V_{oc} for these **P4** based cells was 0.45–0.49 V, reasonably close to the energy difference (~0.6 eV) between the HOMO of **P4** and the LUMO of $PC_{71}BM$. Increasing the weight fraction of $PC_{71}BM$ in the photoactive blend led to a slight decrease in V_{oc}, while J_{sc} was significantly elevated and a PCE of 0.7% was achieved. The unsatisfactory performance might associate with the moderate molecular weight of **P4**, resulting in low conductivity and poor film quality and thus leading to low J_{sc} and FF.

4. Conclusions

Four new low band gap conjugated copolymers **P1–P4** comprising of 3-hexylthiophene (3HT) as the electron-donating unit and 2,3-diethylthieno[3,4-*b*]pyrazine (ETP) as the electron-accepting unit in different molar ratios ranging from 1 : 1 to 4 : 1 were synthesized *via* Suzuki coupling. The introduction of alkyl side chains on each ring allowed all the polymers to exhibit moderate to good solubility in common organic solvents. Increasing 3HT content in the copolymer led to improvements in molecular weights, solubility and thermal stability. Varying the position of the hexyl side chain on 3HT would alter the geometric structure of the copolymer and thus significantly affect the HOMO and the inter-chain packing. The HOMO, ranging from −4.74 eV to −4.88 eV for **P1–P4**, was elevated by increasing the ETP content but was lowered by the break of the co-planarity. The LUMO, ranging from −3.11.eV to −2.94 eV of **P1–P4**, was elevated monotonically with increasing 3HT content. In comparison with pristine P3HT, with only 20 mol% ETP incorporated in **P4**, a pronounced reduction (0.39 eV) in LUMO and a slight elevation in HOMO (0.13 eV) could be achieved. Bimodal UV-vis absorptions with a relative strong absorption at long wavelengths were observed for **P1**, **P3** and **P4** while the ICT absorptions were weaker in **P2**. The optical band gap in solution, ranging from 1.27 eV to 1.76 eV, increased with the increment of 3HT content in the copolymer except **P2**, which was consistent with the variation of the HOMO–LUMO gaps. The particular large band gap and the weaker ICT of **P2** could be attributed to the break of co-planarity in the geometric structure. Theoretical energy levels and optical absorptions were calculated based on density function theory with the B3LYP functional and the 6-31G* basis set were in good agreement with the experimental results, further confirming that the deviation from co-planarity along the main chain would significantly affect the HOMO but would have trivial effect on the LUMO. Therefore, the energy levels and the optical absorptions of the T-TP copolymers could be systematically tuned by adjusting the composition and the geometric structure of the copolymer.

Acknowledgements

The authors would like to thank National Science Council of Taiwan for the financial support from NSC98-2218-E-002-002 and NSC99-2120-M002-011.

References

1 Y. J. Cheng, S. H. Yang and C.-S. Hsu, *Chem. Rev.*, 2009, **109**, 5686.

2 Y. C. Huang, J. H. Hsu, Y. C. Liao, W. C. Yen, S. S. Li, S. T. Lin, C. W. Chen and W. F. Su, *J. Mater. Chem.*, 2011, **21**, 4450.
3 T. W. Zeng, Y. Y. Lin, H. H. Lo, C. W. Chen, C. H. Chen, S. C. Liou, H. Y. Huang and W. F. Su, *Nanotechnology*, 2006, **17**, 5387.
4 L. J. A. Koster, V. D. Mihailetchi and P. W. M. Blom, *Appl. Phys. Lett.*, 2006, **88**, 093511.
5 M. C. Scharber, D. Muhlbacher, M. Koppe, P. Denk, C. Waldauf, A. J. Heeger and C. L. Brabec, *Adv. Mater.*, 2006, **18**, 789.
6 C. J. Brabec, A. Cravino, D. Meissner, N. S. Sariciftci, T. Fromherz, M. T. Rispens, L. Sanchez and J. C. Hummelen, *Adv. Funct. Mater.*, 2001, **11**, 374.
7 A. Gadisa, M. Svensson, M. R. Andersson and O. Inganas, *Appl. Phys. Lett.*, 2004, **84**, 1609.
8 R. Kroon, M. Lenes, J. C. Hummelen, P. W. M. Blom and B. De Boer, *Polym. Rev.*, 2008, **48**, 531.
9 A. Dhanabalan, J. K. J. Van Duren, P. A. Van Hal, J. L. J. Van Dongen and R. A. J. Janssen, *Adv. Funct. Mater.*, 2001, **11**, 255.
10 X. Wang, E. Perzon, J. L. Delgado, P. de la Cruz, F. Zhang, F. Langa, M. Andersson and O. Inganas, *Appl. Phys. Lett.*, 2004, **85**, 5081.
11 O. Inganas, M. Svensson, F. Zhang, A. Gadisa, N. K. Persson and X. Wang, *et al.*, *Appl. Phys. A: Mater. Sci. Process.*, 2004, **79**, 31.
12 L. M. Campos, A. Tontcheva, S. Guenes, G. Sonmez, H. Neugebauer, N. S. Sariciftci and F. Wudl, *Chem. Mater.*, 2005, **17**, 4031.
13 F. Zhang, W. Mammo, L. M. Andersson, S. Admassie, M. R. Andersson and O. Inganas, *Adv. Mater.*, 2006, **18**, 2169.
14 D. Muhlbacher, M. Scharber, M. Morana, Z. Zhu, D. Waller, R. Gaudiana and C. Brabec, *Adv. Mater.*, 2006, **18**, 2884.
15 M. H. Petersen, O. Hagemann, K. T. Nielsen, M. Jorgensen and F. C. Krebs, *Sol. Energy Mater. Sol. Cells*, 2007, **91**, 996.
16 J. Peet, J. Y. Kim, N. E. Coates, W. L. Ma, D. Moses, A. J. Heeger and G. C. Bazan, *Nat. Mater.*, 2007, **6**, 497.
17 M. M. Wienk, M. Turbiez, J. Gilot and R. A. J. Janssen, *Adv. Mater.*, 2008, **20**, 2556.
18 J. Hou, H. Y. Chen, S. Zhang, G. Li and Y. Yang, *J. Am. Chem. Soc.*, 2008, **130**, 16144.
19 E. Zhou, M. Nakamura, T. Nishizawa, Y. Zhang, Q. Wei and K. Tajima, *et al.*, *Macromolecules*, 2008, **41**, 8302.
20 Y. Liang, D. Feng, J. Guo, J. M. Szarko, C. Ray, L. X. Chen and L. P. Yu, *Macromolecules*, 2009, **42**, 1091.
21 Y. Liang, Y. Wu, D. Feng, S. T. Tsai, H. J. Son and G. Li, *et al.*, *J. Am. Chem. Soc.*, 2009, **131**, 56.
22 E. Zhou, J. Cong, K. Tajima and K. Hashimoto, *Chem. Mater.*, 2010, **22**, 4890.
23 E. Zhou, J. Cong, S. Yamakawa, Q. Wei, M. Nakamura and K. Tajima, *et al.*, *Macromolecules*, 2010, **43**, 2873.
24 C. H. Chen, C. H. Hsieh, M. Dubosc, Y. J. Cheng and C. S. Hsu, *Macromolecules*, 2010, **43**, 697.
25 Y. Lee, T. P. Russell and W. H. Jo, *Org. Electron.*, 2010, **11**, 846.
26 K. F. Cheng, C. L. Liu and W. C. Chen, *J. Polym. Sci., Part A: Polym. Chem.*, 2007, **45**, 5872.
27 Y. Zhu, R. D. Champion and S. A. Jenekhe, *Macromolecules*, 2006, **39**, 8712.
28 A. P. Zoombelt, J. Gilot, M. A. Wienk and R. A. J. Janssen, *Chem. Mater.*, 2009, **21**, 1663.
29 M. M. Wienk, M. G. R. Turbiez, M. P. Struijk, M. Fonrodona and R. A. J. Janssen, *Appl. Phys. Lett.*, 2006, **88**, 153511.
30 A. P. Zoombelt, M. Fonrodona, M. G. R. Turbiez, M. M. Wienk and R. A. J. Janssen, *J. Mater. Chem.*, 2009, **19**, 5336.
31 A. P. Zoombelt, M. A. M. Leenen, M. Fonrodona, Y. Nicolas, M. M. Wienk and R. A. J. Janssen, *Polymer*, 2009, **50**, 4564.
32 R. Mondal, N. Miyaki, H. A. Becerril, J. E. Norton, J. Parmer and A. C. Mayer, *et al.*, *Chem. Mater.*, 2009, **21**, 3618.
33 R. Mondal, H. A. Becerril, E. Verploegen, D. Kim, J. E. Norton, S. Ko, N. Miyaki, S. Lee, M. F. Toney, J. L. Bredas, M. D. McGehee and Z. N. Bao, *J. Mater. Chem.*, 2010, **20**, 5823.
34 B. Pal, W. C. Yen, J. S. Yang and W. F. Su, *Macromolecules*, 2007, **40**, 8189.
35 D. D. Kenning, K. A. Mitchell, T. R. Calhoun, M. R. Funfar, D. J. Sattler and S. C. Rasmussen, *J. Org. Chem.*, 2002, **67**, 9073.
36 M. J. T. Frisch, G. W. Schlegel, G. E. Scuseria, M. A. Robb, J. R. Cheeseman, J. A. Montgomery, *et al.*, *Gaussian 03, Revision C.02*, Gaussian Inc, Wallingford CT, 2004.
37 B. C. Lin, C. P. Cheng and Z. P. M. Lao, *J. Phys. Chem. A*, 2003, **107**, 5241.
38 S. Kilina, S. Ivanov and S. Tretiak, *J. Am. Chem. Soc.*, 2009, **131**, 7717.
39 J. B. Foresman, M. Headgordon, J. A. Pople and M. J. Frisch, *J. Phys. Chem.*, 1992, **96**, 135.
40 E. Lim, Y. M. Kim, J. I. Lee, B. J. Jung, N. S. Cho, J. Lee, L. M. Do and H. K. Shim, *J. Polym. Sci., Part A: Polym. Chem.*, 2006, **44**, 4709.
41 G. Tu, S. Massip, P. M. Oberhumer, X. He, R. H. Friend, N. C. Greenham and W. T. S. Huck, *J. Mater. Chem.*, 2010, **20**, 9231.
42 J. Mei, N. C. Heston, S. V. Vasilyeva and J. R. Reynolds, *Macromolecules*, 2009, **42**, 1482.
43 A. Ajayaghosh, *Chem. Soc. Rev.*, 2003, **32**, 181.
44 H. A. M. van Mullekom, J. A. J. M. Vekemans, E. E. Havinga and E. W. Meijer, *Mater. Sci. Eng., R*, 2001, **32**, 1.
45 W. C. Wu, C. L. Liu and W. C. Chen, *Polymer*, 2006, **47**, 527.
46 E. Bundgaard and F. C. Krebs, *Macromolecules*, 2006, **39**, 2823.
47 E. Bundgaard and F. C. Krebs, *Sol. Energy Mater. Sol. Cells*, 2007, **91**, 1019.
48 B. P. Karsten, L. Viani, J. Gierschner, J. Cornil and R. A. J. Janssen, *J. Phys. Chem. A*, 2009, **113**, 10343.